Microfluidic fabrication of tunable alginate-based microfibers for the stable immobilization of enzymes

Wen Zhang[1], Wenbo Ye[1], Ya-Jun Wang[1], and yunfeng Yan[1]

[1]Zhejiang University of Technology

March 21, 2022

Abstract

Immobilized enzymes have drawn widespread attention due to the enhanced stability, easy separation from reaction mixture, and the prominent recyclability. Nevertheless, it is still an ongoing challenge to develop potent immobilization techniques which are capable of stable enzyme encapsulation, minimal loss of activity, and modulability for various enzymes and applications. Here, microfibers with tunable size and composition were fabricated using a home-made microfluidic device. These microfibers were able to efficiently encapsulate bovine serum albumin (BSA), glucose oxidase (GOX) and horseradish peroxidase (HRP). But the physically adsorbed enzymes readily diffused from microfibers into the catalytic reaction system. The leakage of enzymes could be substantially inhibited by conjugating to polyacrylic acid (PAA) and incorporating into the alginate-based microfibers, enabling stable immobilization, improved recyclability, and enhanced thermostability. In addition, GOX and HRP-loaded microfibers were fabricated under the optimized conditions for the visual detection of glucose using the cascade reaction of these enzymes, showing sensitive color change to glucose with concentration range of 0-2 mM. Due to the tunability and versatility, this microfluidic-based microfiber platform may provide a valuable approach to the enzyme immobilization for the cascade catalysis and diagnoses with multiple clinical markers.

Microfluidic fabrication of tunable alginate-based microfibers for the stable immobilization of enzymes

Wen Zhang, Wenbo Ye, Yajun Wang, Yunfeng Yan*

College of Biotechnology and Bioengineering, Zhejiang University of Technology, Hangzhou 310034, China.

* Corresponding author: Yunfeng Yan Email: yfyan@zjut.edu.cn

Data availability statement: Data openly available in a public repository that issues datasets with DOIs

Abstract

Immobilized enzymes have drawn widespread attention due to the enhanced stability, easy separation from reaction mixture, and the prominent recyclability. Nevertheless, it is still an ongoing challenge to develop potent immobilization techniques which are capable of stable enzyme encapsulation, minimal loss of activity, and modulability for various enzymes and applications. Here, microfibers with tunable size and composition were fabricated using a home-made microfluidic device. These microfibers were able to efficiently encapsulate bovine serum albumin (BSA), glucose oxidase (GOX) and horseradish peroxidase (HRP). But the physically adsorbed enzymes readily diffused from microfibers into the catalytic reaction system. The leakage of enzymes could be substantially inhibited by conjugating to polyacrylic acid (PAA) and incorporating into the alginate-based microfibers, enabling stable immobilization, improved recyclability, and enhanced thermostability. In addition, GOX and HRP-loaded microfibers were fabricated under the optimized conditions for the visual detection of glucose using the cascade reaction of these enzymes, showing sensitive color change to glucose with concentration range of 0-2 mM. Due to the tunability and versatility, this microfluidic-based microfiber

platform may provide a valuable approach to the enzyme immobilization for the cascade catalysis and diagnoses with multiple clinical markers.

Keywords

Immobilized enzyme, microfluidics, microfiber, glucose oxidase, sodium alginate

Introduction

The increasing importance of industrial biocatalysis has led to the extensive development of heterogeneous biocatalysts employing immobilization technologies (Rudroff et al., 2018). The rational design of stable, active, and reusable immobilized enzymes is an urgent need for the broad application of industrial enzymes. So far, the immobilization of enzymes is a facile and economically feasible strategy to improve their stability and reusability through a variety of methods such as entrapment, encapsulation, adsorption, crosslinking, and covalent attachment to water-insoluble matrices (Basso & Serban, 2019; Bayramoglu & Arica, 2008; Bilal et al., 2019; Cantone et al., 2013; Liese & Hilterhaus, 2013; Liu et al., 2018). Substantial progresses have been made in the development of enzyme immobilization in recent years. Nevertheless, the practical application of a large number of immobilized biocatalysts still suffers from varying problems, e.g., enzyme leaching, low stability, limited diffusion, deactivation, sophisticated recycling, which reduces the catalytic efficiency and hinders their industrial application (Bilal & Iqbal, 2019; Liang et al., 2020; Secundo, 2013; Zhou & Hartmann, 2013). The exploration of appropriate supporting matrix and novel technologies for enzyme immobilization has attracted intensive attentions (Grant et al., 2018; He et al., 2020; Henderson et al., 2019; Ho et al., 2019; Jannat & Yang, 2020; Ko et al., 2019; Liang et al., 2020; Liu & Nidetzky, 2021; Ren et al., 2019; Teepakorn et al., 2021; Yang et al., 2020; Zanker et al., 2021; Zhu et al., 2019b).

Microfluidic platform is a promising technique for manufacturing customizable structures integrating with rapid crosslinking strategies (Hu et al., 2020; Huang et al., 2020; Jeong et al., 2004; Jun et al., 2014; Ren et al., 2019; Shao et al., 2019; Teepakorn et al., 2021). The convergence of the emerging microfluidic technology and materials science enables novel applications in varying fields including enzyme immobilization (Ho et al., 2019; Kabernick et al., 2022; Teepakorn et al., 2021; Zhu et al., 2019b). Alginate is a natural biomaterial that widely used in immobilization of protein/enzyme, drug, and cell because of the rapid crosslinking by multivalent cations (e.g., Ca^{2+} or Ba^{2+}) (Bedade et al., 2019; Cheng et al., 2014; Jeon et al., 2009; Kahya & Erim, 2019; Pawar & Edgar, 2012; Qin, 2008; Yu et al., 2017). Alginate-based microfibers, microspheres, and microparticles can be feasibly fabricated via microfluidics technique which are widely used in fundamental researches and practical applications (Cheng et al., 2014; Jeong et al., 2004; Jun et al., 2014; Pawar & Edgar, 2012; Qin, 2008; Shin et al., 2007; Yu et al., 2017). They are capable of modifying or blending with other organic or inorganic materials for the immobilization of protein/enzyme (Bedade et al., 2019; Coppi et al., 2002; Lee & Lee, 2016; Wang et al., 2011; Wu et al., 2015), controlled release of protein drug (Kahya & Erim, 2019), or the detection of alkaline phosphatase, hydrofluoric acid, lactate, glucose (Gunatilake et al., 2021; Lee & Lee, 2016; Li et al., 2019). It has been reported that the calcium-crosslinked alginate hydrogel possesses a microporous structure, which benefits the rapid diffusion of substrates and products during catalysis while leads to the leakage of physically adsorbed enzymes from the matrix as well (Shao et al., 2018; Zdarta et al., 2018). To address this challenge, covalent binding or crosslinking was introduced to enzyme immobilization to improve the stability and suppress enzyme leaching (Jannat & Yang, 2020; Sheldon & van Pelt, 2013). In addition, the microfluidic fabrication endows alginate microfibers with flexible manipulation on the diameter, composition, and pore size of microfibers, which plays a substantial role in the development of supports for enzymes with specific physicochemical features (Cheng et al., 2014; Jun et al., 2014; Yu et al., 2017; Zhu et al., 2019b).

In this study, we developed co-flow microfluidic devices for the fabrication of alginate-based microfibers in coaxial glass capillaries. This approach is capable of fine tuning the diameter and crosslinking degree of microfibers. Moreover, alginate microfibers with covalently bound enzymes were readily constructed and easily collected using this microfluidic platform, showing excellent reusability and improved thermal stability. After loading with glucose oxidase and horseradish peroxidase, the alginate microfibers are able to sense

glucose in a wide range of concentrations (**Scheme 1**). Due to the feasible modulation of the physicochemical properties of microfibers, the microfluidic platform may have great potential in the construction of microfiber carriers for enzyme immobilization and multitarget detection.

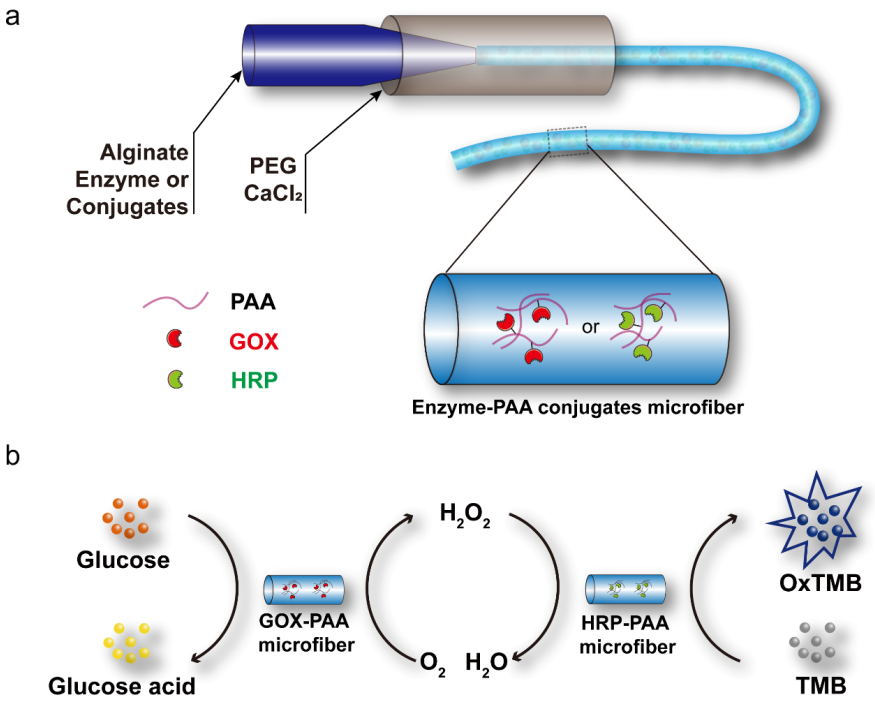

Scheme 1 (a) Schematic illustration of the enzyme-immobilized alginate microfibers and (b) colorimetric detection of glucose by microfibers.

Materials and methods

2.1 Materials

Sodium alginate, calcium chloride (dihydrous) and poly (acrylic acid) (PAA) solution were purchased from Sigma-Aldrich (USA). 1-Ethyl-3-(3-dimethylaminopropyl) carbodiimide hydrochloride (EDC·HCl) and N-hydroxy succinimide (NHS) were purchased from Aladdin Chemistry (China). Glucose oxidase (GOX) from *Aspergillus niger* was obtained from Solarbio (China). Horseradish peroxidase (HRP), 3,3',5,5'-tetramethylbenzidine (TMB), and dimethyl sulfoxide (DMSO) were purchased from Sangon Biotech (China). Bovine serum albumin (BSA) was obtained from Beyotime (China). Fluorescein-5-isothiocyanate (FITC) was purchased from Thermo Fisher Scientific (USA). Triethylamine was obtained from Shanghai Lingfeng Chemical Reagent (China). Poly (Ethylene Glycol) (M_n = 400 Da) was purchased from Greagent (China).

2.2 Preparation of the microfluidic device and microfibers

The microfluidic device was built up by coaxially aligning two cylindrical capillaries (1 mm outer diameter (O.D.) and 0.58 mm inner diameter (I.D.)) inside a square capillary (1 mm I.D.) according to previous reports (Cheng et al., 2014; Othman et al., 2015; Yu et al., 2018). First, the square capillary was fixed onto a glass slide with epoxy glue. The cylindrical capillary was tapered using a capillary puller (PC-100, Narishige, Japan) and subsequently shaped using a microforge (MF-900, Narishige, Japan) to desired orifice (60 or 150 μm I.D.). Then, the tapered cylindrical capillary was inserted into another untapered cylindrical capillary in the fixed square capillary on the glass slide. At last, two syringe needles (2.5 mm O.D. and 0.9 mm I.D.) with plastic hubs were placed onto the junction between the cylindrical capillaries and square capillary followed by sealing the gap with epoxy resin.

The alginate (2%, w/v) solution was pumped using a syringe pump (SLP01-02A, Longer, China) into the tapered round capillary while the outer phase (50% PEG and 2% $CaCl_2$) was pumped by another pump (SLP01-01A, Longer, China) in the identical direction through the region between the inner cylindrical capillary and outer square capillary. Straight microfibers were easily fabricated in the channel via the effective and rapid crosslinking of Ca^{2+} and alginate (Yu et al., 2017). The diameter and composition of alginate-based microfibers were readily modulated by adjusting the diameter of tapered orifice, flow rate, and the concentration of the inner or outer phases (Yu et al., 2018). Free BSA, enzymes, or their conjugates with PAA were added to alginate solution for fabricating protein/enzyme-loaded microfibers using similar protocol. Microfibers were collected by wrapping on paper clips for catalysis assays.

Encapsulation of BSA in microfibers 2.3.1 Encapsulation efficiency of BSA BSA-loaded microfibers were prepared using the internal phase containing alginate (2%, w/v) and BSA (5, 10, 15, 20, 25, 30, 35, 40 mg/mL). The mixture of BSA and alginate was centrifuged (4000 rpm, 1 min) to remove air bubbles prior to the preparation of microfibers. BSA concentration was determined by the Bradford assay method. The encapsulation efficiency (EE) and loading capacity (LC) were calculated according to equations (1) and (2) (Kahya & Erim, 2019): $EE\% = \frac{m0-m1}{m0} \times 100$ (1) $LC\% = \frac{m0-m1}{m0+m2-m1} \times 100$ (2) Where m_0 is the feeding mass of BSA in the preparation of microfibers, m_1 is the mass of free BSA, m_2 is the mass of alginate in microfibers.

2.3.2 BSA release studies

BSA-loaded alginate microfibers were prepared under selected conditions (the flow rate of inner phase: 0.2 mL/h, the flow rate of out phase: 17 mL/h) and collected for 10 min. Microfibers were immersed in 1 mL deionized water in microcentrifuge tube and shaken (90 rpm) at room temperature. At each time interval (60 min), 20 μL release media was taken for BSA concentration assays, to which 20 μL fresh water was added to the centrifuge tube to keep the volume constant (Kahya & Erim, 2019). BSA content in the samples was determined by the Bradford protein assay at 595 nm and measurements were performed with a microplate reader (spectraMAX M5, Molecular Devices, USA). All experiments were performed in triplicate.

Synthesis of enzyme-polymer conjugates

Carboxyl groups of PAA were activated by EDC/NHS coupling reaction followed by the addition of GOX for the covalent attachment of enzymes to PAA (Grabovac et al., 2015; Riccardi et al., 2014; Zore et al., 2017). Specific steps are as follows: a stock solution of PAA was prepared by dissolving 0.893 g PAA (35%) in 7 mL deionized water. 0.833 g EDC and 0.25 g NHS were dissolved in 1 mL water and added dropwise into the PAA solution. The mixture was gently stirred at room temperature for 18 h after the pH was adjusted to 7.4 by adding triethylamine. 1 mL GOX solution (10 mg/mL) was added dropwise into the above mixture and the mixture was stirred for 6 h. GOX-PAA conjugates solution with GOX concentration of 1 mg/mL was successfully prepared after dialysis with cellulose membrane (molecular weight cut-off of 200 kDa) against deionized water for the following studies (Ji et al., 2017; Zore et al., 2017). Other enzyme-PAA conjugates (HRP-PAA) were synthesized using the same protocol and mixed with alginate for the fabrication of enzyme-immobilized microfibers (Riccardi et al., 2014). The covalent conjugates were confirmed with FTIR spectroscopy (Nicolet 6700 FTIR-ATR analyzer, Thermo Fisher Scientific, USA). The spectra were recorded in the range of 4000–400 cm^{-1} with a resolution of 1.0 cm^{-1} at room temperature.

2.5 Characterization of microfibers

The formation of microfiber was monitored using an optical microscope with digital camera (LW300LT, Cewei Optoelectronics Technology Co., Ltd., China). The diameter of microfibers was measured using the included software of the microscope. FITC-labeled BSA (FITC-BSA) was prepared according to previous reports (Kizilay et al., 2014; Zhang et al., 2010). Fluorescence images of the FITC-BSA encapsulated microfibers were recorded using an Axio Observer A1 fluorescence microscope (Carl Zeiss Inc., Germany). The morphologies of fibers were observed using Scanning Electron Microscopy (GeminiSEM500, Zeiss, Germany). The SEM images were taken using in-lens detector operating at an accelerating voltage of 5 kV and a working distance of 5.5 mm.

2.6 Activity assay of enzymes

2.6.1 Activity assay of GOX

GOX catalyzes the conversion of glucose to glucuronic acid ($C_6H_{12}O_7$), producing hydrogen peroxide (H_2O_2) simultaneously. Upon reacting with H_2O_2, the colorless substrate TMB is readily converted to the oxidized TMB (OxTMB) which has a maximum absorption at 652 nm (Lin et al., 2014; Singh et al., 2017). Hence, the catalytic activity of GOX was evaluated by the measurements of the consumption of glucose based on these reactions. Specific steps are as follows: 0.2 mL of glucose solution (5 mM), 0.02 mL of HRP solution (10 mg/mL), and 2.15 mL phosphate buffer (10 mM, pH 6) were mixed in a glass cuvette followed by the quick addition of 0.05 mL of the GOX enzyme solution (0.5 mg/mL) or immobilized enzyme. After 2 min-equilibration, UV absorption (652 nm) was measured. A unit of GOX activity is defined as the amount of enzyme which oxidizes 1.0 μmol of β-D-glucose to gluconic acid and H_2O_2per minute (Wang et al., 2011).

2.6.2 Activity assay of HRP

HRP converts guaiacol to tetraguaiacol (maximum UV absorption at 470 nm) in the presence of H_2O_2. The activity of HRP can be evaluated by measuring the absorbance change at 470 nm (El-Naggar et al., 2021; Felisardo et al., 2020; Liu et al., 2021). Specific steps are as follows: 2.85 mL of phosphate buffer solution, 0.05 mL of H_2O_2 solution (0.3 %), and 0.1 mL of guaiacol solution (0.02 mol/L) were added in a glass cuvette (1 cm width) followed by the quick addition of 0.05 mL of the enzyme solution or immobilized HRP. The UV absorption (470 nm) of the mixture was recorded after equilibrating for 2 min. The activity unit of HRP is defined as the amount of the enzyme which increases the absorption value by 1.0/min under corresponding assay conditions (El-Naggar et al., 2021).

2.7 Evaluation of the enzyme-immobilized microfibers

2.7.1 pH dependent catalysis

The GOX-PAA immobilized microfibers were collected for 10 min using the following parameters: the tapered orifice was 60 μm, the flow rate of inner phase (2% alginate, 0.5 mg/mL GOX-PAA) and outer phase (50% PEG, 2% $CaCl_2$) were 0.2 mL/h and 17 mL/h, respectively. The activity of free and immobilized GOX-PAA was tested in different buffers (10 mM, pH 4.0–9.0) at room temperature to assess the optimum pH. The relative activity of enzyme-immobilized microfibers at varying pHs was normalized to that of microfibers with the optimum pH.

2.7.2 Temperature dependent catalysis

The enzyme-immobilized microfibers were collected for temperature dependent assay using the parameters mentioned above. The temperature dependent catalysis of free and immobilized GOX-PAA were assayed at 40-70 °C to assess the optimum temperature. For the thermal stability studies, the microfibers or free enzymes were incubated at 40 °C, 50 °C, 60 °C, or 70 °C for 30, 60, or 90 min, followed by immediately cooling to room temperature for catalytic activity assays. The relative activity of microfibers was normalized to that of without thermal treated microfibers.

2.7.3 Reusability of immobilized enzymes

The reusability of enzyme-immobilized microfibers means the capability of the immobilized GOX to be used for repeated cycles. For this study, microfibers were immersed in a solution containing 0.2 mL of glucose solution (5 mM), 0.02 mL of HRP solution (10 mg/mL), and 2.15 mL buffer (10 mM, pH 6) in a glass cuvette. After the reaction at room temperature for 10 min, the microfibers were taken out from the cuvette and TMB solution was added to the reaction mixture. Then microfibers were washed with deionized water, and added to the fresh reaction mixture subsequently. The catalytic activity of microfibers was evaluated by the analysis of the residual glucose in the reaction solution according to the protocol mentioned above. The relative activity of microfibers at each cycle was normalized to that at the first cycle.

2.8 Visual detection of glucose using enzyme-loaded microfibers

For the sensitive detection of glucose, the weight ratio of HRP and GOX in the microfibers was optimized by changing the composition of the inner phase in the preparation of HRP and GOX-loaded microfibers. The total enzyme content was kept constant and the weight ratios of HRP to GOX (W_{HRP}/W_{GOX}) were 8:1, 4:1, 2:1, 1:1, 1:2, 1:4, or 1:8.

0.1 mL TMB DMSO solution (12 mM) was added dropwise to the mixture containing 0.5 mL alginate (2%, w/v), 0.2 mL GOX, and 0.2 mL HRP (10 mg/mL) in a 5 mL beaker. The blend was gently stirred for 30 minutes until it became homogeneous, and used as the inner phase. Enzymes and TMB-loaded microfibers for glucose detection were prepared and collected using the method mentioned above. For the detection of glucose, 20 μL glucose solution (10 mM PBS, pH 6) with various concentrations (0, 0.25, 0.5, 1, 2 mM) was added onto the wrapped microfibers. The color of microfibers readily changed from light golden to blue with varying degrees, depending on the concentration of glucose.

Results and discussion3.1 Preparation of microfibers and encapsulation of protein/enzyme Using the home-made microfluidic device, the straight alginate-based microfibers was formed continuously due to the feasible gelation upon the rapid crosslinking of alginate with Ca^{2+}(**Fig. S1)** . The addition of PEG into $CaCl_2$solution increased the viscosity of the external phase, suppressing the diffusion of alginate flow and benefiting the stable formation of microfibers (Yang & Guo, 2019; Zhu et al., 2019a). Moreover, the diameter of alginate microfibers increased from 21.1 to 90.7 μm with the decrease of the flow rate of outer phase from 28 to 5 mL/h when the flow rate of alginate was kept constant at 0.2 mL/h and the inner diameter of orifice was 60 μm (**Fig. S2)** . Under these experimental settings, the higher flow rate of the outer phase stretched the alginate stream at the constant flow rate of inner phase, leading to smaller diameter of microfibers. Further increasing the flow rate of the outer phase ultimately resulted in the break of microfibers while too low flow rate of the outer phase led to clogging the microfluidic channel. Thicker microfibers could be fabricated using the microfluidic device with larger orifice dimension under proper conditions. For example, microfibers with the diameter of 100 μm could be prepared when the orifice was 150 μm, the flow rate of outer phase and inner phase were 18 and 0.5 mL/h, respectively. It was obviously that fluids mainly form laminar flow under the above conditions.

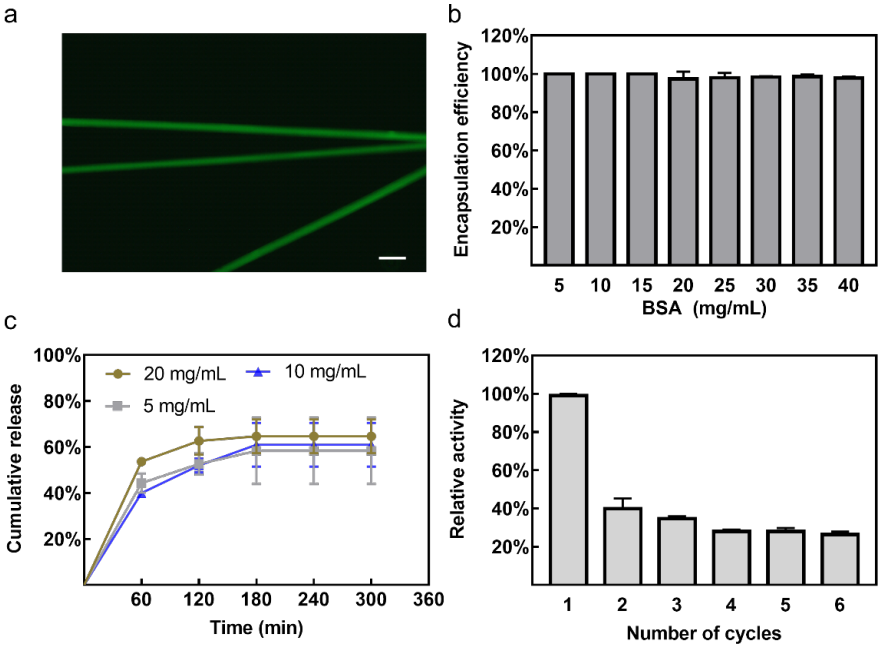

Fig. 1 Immobilization of BSA or GOX in alginate-based microfibers. (a) Fluorescence imaging of FITC-BSA loaded microfibers. Scale bar = 100 μm. (b) Encapsulation efficiency of BSA in microfibers. (c) Cumulative

release of BSA from the microfibers. (d) Relative activity of the encapsulated GOX (mean ± SD, n = 3).

To check the feasibility of microfibers for enzyme immobilization, BSA was used as a model to measure the protein loading capacity and release behavior of protein-encapsulated microfibers because BSA shows similar pI to GOX (Singh et al., 2014; Zore et al., 2017). Fluorescence images of FITC-BSA loaded microfibers demonstrated the successful encapsulation of protein, suggesting the potential for the immobilization of enzymes (**Fig. 1a**). The EE of BSA in the selected microfibers at varying feeding concentrations was higher than 95% (**Fig. 1b**). The BSA loading capacity (LC) of microfibers increased with BSA content in the inner phase (**Fig. S3**). When the concentration of feeding BSA was 40 mg/mL, the LC was as high as 66%, indicating the excellent performance for protein loading. However, BSA was readily released from the microfibers which were constructed by the physical encapsulation of BSA in the alginate blend when the microfibers were incubated with deionized water (**Fig. 1c**). There were only 35%-40% proteins remaining in the microfibers after 3 h incubation. During the preparation of microfibers, the concentrate PEG outer phase was able to constrain the alginate stream and suppress the diffusion of BSA from the inner phase. When the microfibers were transferred to deionized water, loosely bound BSA was prone to diffuse across the macropore of alginate fibers to aqueous phase (Gao et al., 2015; Kahya & Erim, 2019). The leakage of physically adsorbed proteins was further confirmed by the catalytic assays of GOX-loaded microfibers (**Fig. 1d**). The relative activity of microfibers decreased to 30% after reuse for 3 times.

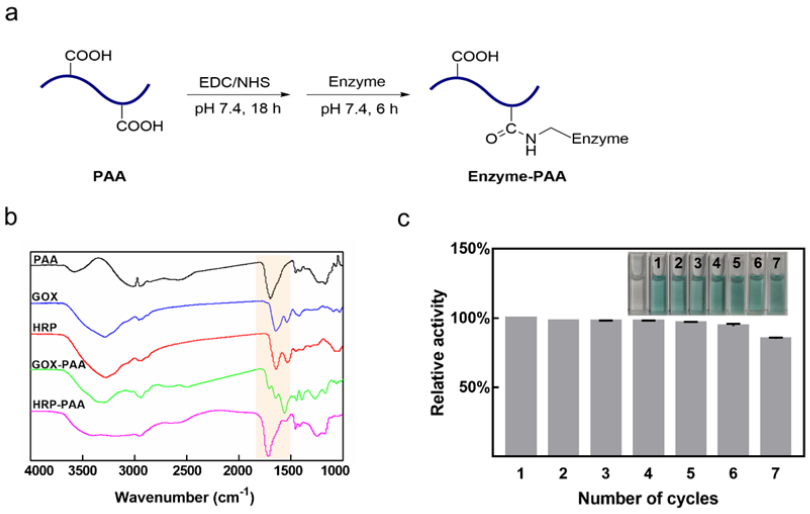

Fig. 2 Preparation and the catalytic activity of microfibers based on alginate and enzyme-PAA conjugates. (a) Synthesis of enzyme-PAA conjugates. (b) FT-IR spectra of PAA, GOX, HRP, GOX-PAA conjugate, and HRP-PAA conjugate. (c) Reusability of GOX-PAA immobilized alginate microfibers.

To reduce the leakage from microfibers, enzymes were conjugated to PAA prior to mix with alginate for microfluidic fabrications (**Fig. 2a**). FTIR spectroscopy was utilized for the analysis of enzyme-PAA conjugates (Nie et al., 2005). The FTIR spectra of PAA showed typical absorption of COOH at 1702 cm^{-1} which corresponds to the stretching vibration of C=O bonds while the spectra of enzymes showed absorption of amide I and II at 1634 cm^{-1} and 1538 cm^{-1}, respectively (**Fig. 2b**). After coupling reaction and subsequently dialysis, the IR spectra of resulting mixture of PAA and enzymes demonstrated the coexistence of the characteristic absorption of the starting components, indicating the successful preparation of enzyme-PAA conjugates (Gejji & Fernando, 2018). It is worth noting that enzyme-alginate conjugates cannot be prepared via EDC/NHS coupling strategy (**Fig. S4**). The enzyme cannot covalently bind to alginate which may be ascribed to the steric hindrance of the cyclic structure to the coupling reaction on the COOH of alginate. Abundant carboxyl groups in the flexible PAA enables not only the feasible conjugation with

proteins but also the robust chelation with Ca^{2+} which is beneficial for the formation of microfibers and the immobilization of enzymes in the fibers.

By the covalent attachment to Ca^{2+}-crosslinkable PAA, the leakage of enzymes was inhibited and the reusability of the enzyme-immobilized microfibers was substantially improved (**Fig. 2c**). The insert images showed that the color of solution after catalysis reaction with GOX-immobilized microfibers did not change significantly in the first to the seventh use, indicating the consistent catalytic activity of enzymes in microfibers during these reactions. The quantitative data showed that the immobilized GOX-PAA retained over 85% of its initial activity after seven cycles of utilization. The highly remained activity could be attributed to the firm attachment of enzymes to PAA and the robust crosslinking of alginate and GOX-PAA with Ca^{2+}, which leads to efficacious prevention of enzyme from leakage during the enzymatic reaction. These microfibers were capable of ease collection and handling, as well as modulatable size and component, thus, offering promising potential in enzyme immobilization for multiple purposes.

3.2 Characterization of alginate-based microfibers

SEM images of alginate microfibers with diameter of 50 and 100 μm (the size measured by optical microscope during microfluidic fabrication) showed that the microfibers had smooth surfaces and the change of preparation settings (e.g., the flow rate and the inner diameter of capillary) did not remarkably affect the morphologies of microfibers (**Figs. 3a** and **3b**). The rapid chelation of sodium alginate with calcium ions at the orifice of tapered aperture, and the high viscosity of PEG solution may suppress the diffusion of alginate from the inner phase to the outer phase, leading to the formation of smooth surfaces. Moreover, the size of dry microfibers observed by SEM was consistent with that at swollen state measured by optical microscope in the preparation of microfibers, indicating the robust crosslinking in the microfibers and no significant shrinkage during drying for SEM observation.

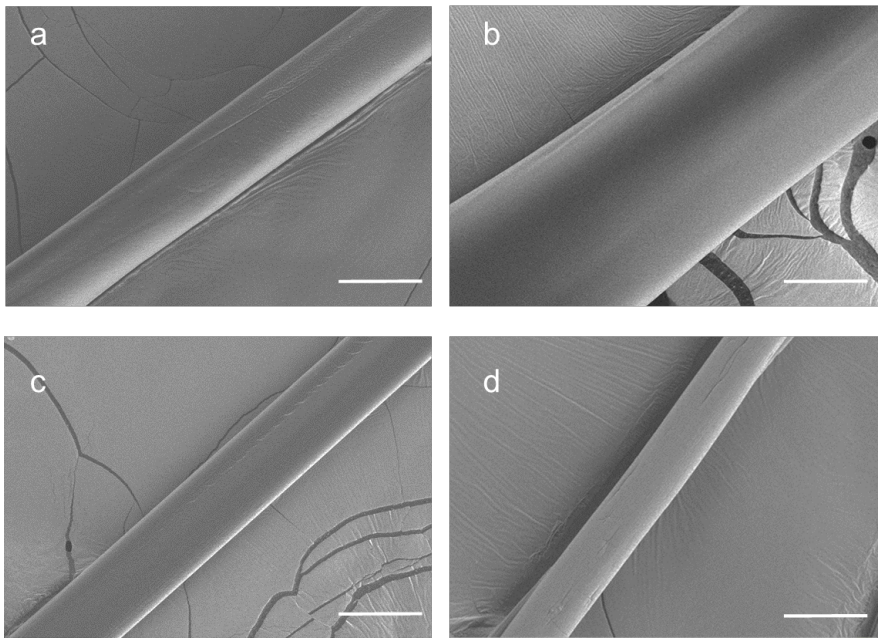

Fig. 3 Scanning electron microscopy (SEM) images of microfibers. (a) and (b) SEM images of microfibers with the diameter of 50 and 100 μm prepared with alginate only. (c) and (d) SEM images of GOX-PAA immobilized alginate microfibers before catalysis use and after six cycles of utilization. Scale bar = 50 μm.

The diameter and surface topography of microfibers did not change when GOX-PAA was added into alginate phase (**Fig. 3c)** . After repeating use for 6 cycles, the diameter decreased by ˜10 μm but the integrity of

microfibers remained (**Fig. 3d)** . The shrinkage in size may be ascribed to the slight dissociation of enzymes, enzyme-PAA, or alginate and the reorganization of instantaneously crosslinked polymer-protein blends during the catalysis reaction. In general, the microfibers composed of alginate and enzyme-PAA held outstanding stability and reusability for enzyme immobilization.

3.3 Effects of diameter and alginate content on the catalytic activity of microfibers

One of advantages of the microfluidic fabrication of microfibers is the capability of tuning the diameter and the composition of microfibers, which affect the catalytic performance of immobilized enzymes. Here we prepared microfibers with different diameters or alginate contents and tested the catalytic activity at the same enzyme concentration. The catalytic ability of HRP-PAA immobilized microfibers could be demonstrated with the kinetics of the conversion of guaiacol into tetraguaiacol (Felisardo et al., 2020). Figures 4a and 4c showed that enzyme-loaded microfibers with the diameter of 50 μm enabled more rapid increase in the color and the absorption at 470 nm comparing with the thicker ones (100 μm), suggesting more efficient conversion of guaiacol into tetraguaiacol by the catalysis with thinner microfibers at the same amount of HRP. The diffusion barriers of substrates and products decreased with the diameter of microfibers, therefore facilitating the mass exchange between the intra-microfiber and the aqueous phase for thinner microfibers. Moreover, the relative surface area of thinner microfibers is larger that of thicker microfibers, which is beneficial for the catalytic reaction.

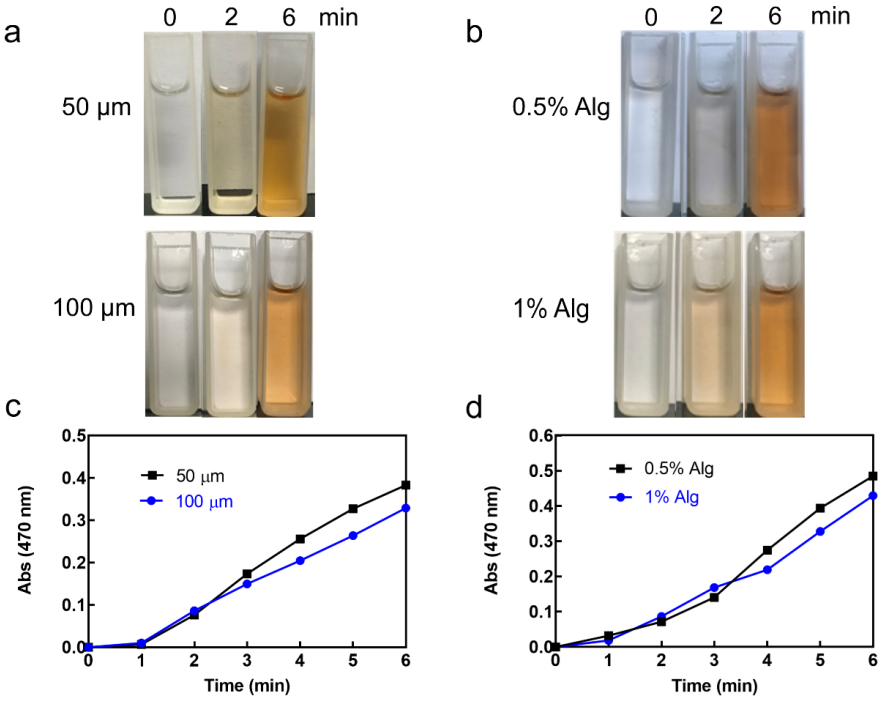

Fig. 4 Catalytic kinetics of HRP-PAA immobilized alginate microfibers with different diameters or alginate contents. (a) Photos of substrate solution after catalysis with microfibers of 50 or 100 μm. (b) Photos of substrate solution after catalysis with microfibers prepared with 0.5% or 1% alginate. (c) Time dependent absorption (470 nm) of substrate solution after catalysis with microfibers of 50 or 100 μm. (d) Time dependent absorption (470 nm) of substrate solution after catalysis with microfibers prepared with 0.5% or 1% alginate.

We then prepared two kinds of microfibers with the same diameter (50 μm) and enzyme content but different alginate contents. The catalytic efficiency of HRP-immobilized microfibers was analyzed by the color observation and absorption at 470 nm (**Figs 4b** and **4d**). Data showed that microfibers prepared with 1% alginate demonstrated slightly lower catalytic activity those prepared with 0.5% alginate. More alginate in

the inner phase of preparation led to more crosslinking and compact internal structure of microfibers, which may hinder the exchange of substrates and products during catalysis. However, the mechanical property of microfibers dramatically decreased with the content of alginate. A higher alginate content is usually required for the fabrication of stable microfibers for reuse.

3.4 Effects of pH and temperature on the catalytic activity of microfibers

The pH dependent catalytic activities of free and immobilized GOX were studied at pH 4-9. **Fig. 5a** showed that free and immobilized GOX-PAA exhibited optimum pH at 4 and 6, respectively, which is similar to the report in the literature (Todea et al., 2021). The additional interaction between GOX and alginate or PAA, in particular electrostatic interaction is pH dependent. The catalysis-related conformation of GOX-PAA may be altered with pH, resulting in different optimal pH for free and immobilized enzymes (Bedade et al., 2019; Hanefeld et al., 2009).

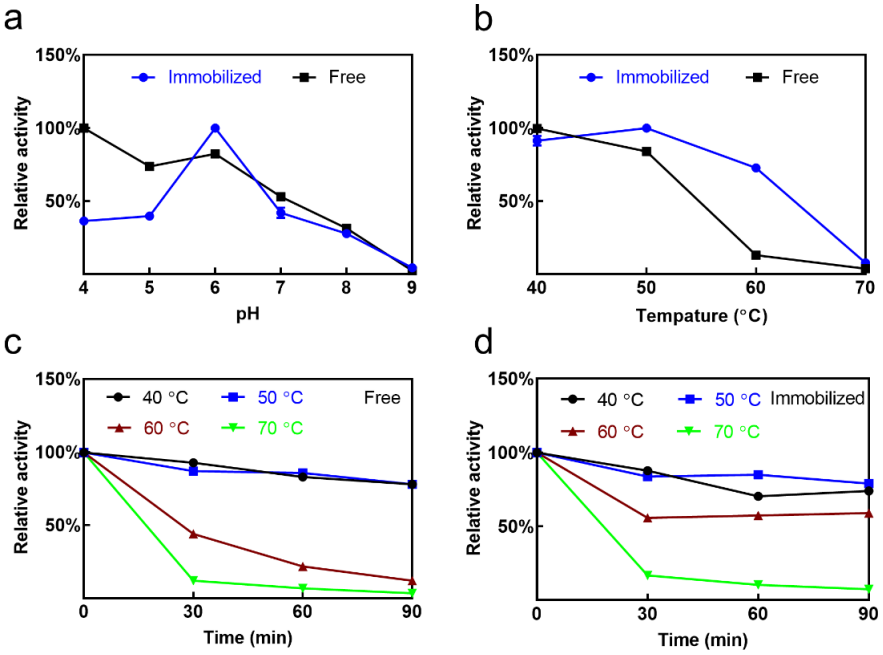

Fig. 5 pH and temperature dependence of catalysis with free or immobilized GOX. (a) The relative catalytic activity of free or immobilized enzymes at pH 4-9. (b) The relative catalytic activity of free or immobilized GOX at 40-70 °C. (c) The relative catalytic activity of free GOX after heating at 40 °C, 50 °C, 60 °C, or 70 °C for 0-90 min. (d) The relative catalytic activity of immobilized GOX after heating at 40 °C, 50 °C, 60 °C, or 70 °C for 0-90 min.

Temperature is one of the key factors for the catalysis reaction and the stability of enzymes. **Fig. 5b** showed that the catalytic activity of both free and immobilized GOX decreased with temperature above 50 °C. For the immobilized GOX, the decrease of activity was much slower than that of free GOX, indicating better tolerance of immobilized enzymes to heating. The favorable ability of resistance to thermal inactivation for the immobilized enzymes may ascribed to the protection of the alginate carriers. The thermal stability of immobilized enzymes was further investigated by the catalysis assays of enzyme-loaded microfibers after heat treatments at different temperature for 0-90 min (**Figs. 5c**and **d**). For the heat treatments at 40 °C and 50 °C, immobilized GOX exhibited moderate decrease in the relative catalytic activity with the increase of heating time, which is similar to that of free GOX. Meanwhile, heating at 70 °C readily resulted in the substantial inactivation of both free GOX and immobilized GOX. For the heat treatment at 60 °C, enzyme-immobilized microfibers retained about 60% of the catalytic activity after heating for 60 and 90 min

whereas the relative catalytic activity of free GOX was less than 20% under the same conditions. The results demonstrated that the thermal stability of immobilized enzymes in alginate-based microfibers was enhanced due to the increased rigidity of enzyme caused by the firm attachment to microfibers and the protection of alginate matrix for enzymes (Bedade et al., 2019; Todea et al., 2021; Zhang et al., 2015).

3.5 HRP and GOX co-immobilized microfibers for the visual detection of glucose

Besides the excellent thermal stability and recyclability of the immobilized enzymes, microfluidic fabrication endowed alginate-based fibers with tunable composition and size as well as good mechanical properties for knitting, which suggests the potential applications in the construction of detection chips on demand. To validate this potential, microfibers loaded with HRP, GOX, and the chromogenic substrate TMB were prepared under the optimal conditions and wrapped on a glass slide for the visual detection of glucose (**Fig. 6**). By the catalysis with GOX, glucose could be oxidized to gluconic acid in aqueous solution while oxygen was simultaneously converted to H_2O_2. which oxidizes TMB to a green-blue product OxTMB in the presence of HRP (**Scheme 1b**) (Dong et al., 2012; Lin et al., 2014; Ren et al., 2019).

First, the weight ratio of GOX-PAA and HRP-PAA was optimized to improve the catalytic efficiency of the multi-enzyme immobilized microfibers. When the total amount of GOX and HRP was constant, the conversion of TMB to OxTMB increased with GOX as HRP/GOX weight ratio decreased from 8:1 to 1:2. Because the molecular weight of GOX is about 4 times as that of HRP, the molar ratio of HRP to GOX was about 32:1 to 2:1, suggesting that the chromogenic reaction was dominated by the catalysis with GOX under these conditions. More GOX improved the oxidation of glucose and the subsequent conversion of TMB to OxTMB in the presence of abundant HRP. Further increase of GOX did not improve the chromogenic reaction due to the decrease of HRP when HRP/GOX weight ratio was lower than 1:2 (**Fig. 6a**). In general, enzymes co-immobilized microfibers exhibited obvious absorption for the successive reactions at HRP/GOX weight ratio of 1:1 to 1:8. These microfibers showed great GOX activity at the ratio of 4:1 to 1:2 (**Fig. S5**). HRP and GOX with equivalent weight were selected for the preparation of enzyme-loaded microfibers for glucose detection.

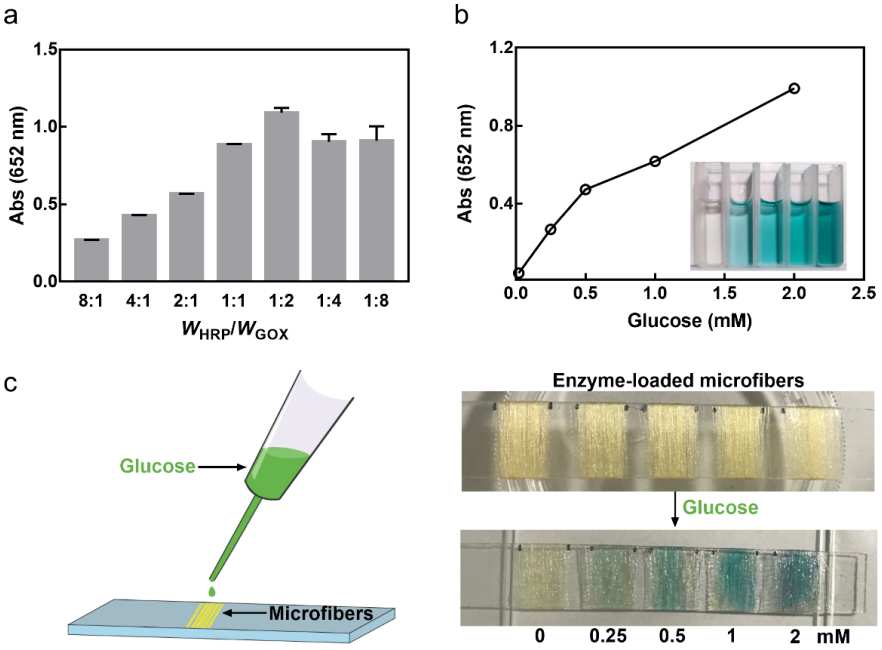

Fig. 6 Glucose detection with enzyme-loaded microfibers. (a) The effect of HRP/GOX weight ratio on the absorption of mixture of glucose and TMB after catalysis with HRP and GOX-loaded microfibers. (b) The

effect of glucose concentration on the absorption of the aqueous solution containing enzymes, glucose, and TMB. (c) Visual detection of glucose (0, 0.25, 0.5, 1, 2 mM) with enzymes and TMB-loaded microfibers.

Prior to the glucose analysis with microfibers, the chromogenic reaction in aqueous solution were investigated at selected concentrations of glucose (**Fig. 6b**). Data showed that the absorption (652 nm) of the mixture increased with glucose concentration. But the relationship between the absorption and the concentration was not linear in the selected range of glucose concentration. The slope of the curve was smaller when the glucose concentration was higher than 2 mM, indicating that the color change was less sensitive to glucose with too high concentrations. For visual detection of glucose, microfibers with enzymes and TMB were fabricated under the optimal conditions and wrapped on a glass slide (**Fig. 6c**). The aligned fibers turned to blue after dropwise adding with 20 μL of glucose solution. The blue color remarkably became deeper with the increase of glucose concentration from 0 to 2 mM. The catalysis reaction was triggered by the addition of glucose and the penetration into the pores of the hydrogel network followed by the rapid generation of OxTMB, which causes the visible blue color in the microfibers. The knittability and the modulability in the composition and size enabled great potentials of the microfluidic microfibers in the construction of portable devices for the simultaneous detection of multiple markers.

4. Conclusions

In this study, a home-made co-flow microfluidic chip was constructed to prepare the alginate-based microfibers which composition, size, and degree of crosslinking was feasibly tunable. These microfibers were capable of effectively absorbing BSA and enzymes. To reduce the leakage of enzymes from microfibers in the catalytic reaction solution, GOX was covalently grafted to PAA and formed microfibers with alginate. The resulting microfibers enabled stable encapsulation and excellent repeating use of enzymes. Over 85% of the activity remained after seven cycles of reuse. Moreover, GOX-PAA immobilized microfibers exhibited enhanced thermostability than free GOX. Two enzymes (GOX and HRP) were loaded in microfibers for the visual detection of glucose using the cascade reaction of these enzymes. The enzyme ratio-optimized microfibers demonstrated rapid and sensitive color change upon addition of glucose with concentration of 0-2 mM. Due to the feasibility and tunability, this versatile microfiber platform may have great potential in the immobilization of various enzymes for catalysis and simultaneous detection of multiple diagnostic markers.

Acknowledgements

This work was supported by the National Natural Science Foundation of China (U1932164), the Zhejiang Provincial Natural Science Foundation (LY19B040004).

References:

Basso, A., Serban, S. (2019). Industrial applications of immobilized enzymes—A review. *Molecular Catalysis* , 479, 110607. https://doi.org/10.1016/j.mcat.2019.110607

Bayramoglu, G., Arica, M.Y. (2008). Enzymatic removal of phenol and p-chlorophenol in enzyme reactor: horseradish peroxidase immobilized on magnetic beads. *Journal of Hazardous Materials* , *156* (1-3), 148-155. https://doi.org/10.1016/j.jhazmat.2007.12.008

Bedade, D.K., Sutar, Y.B., Singhal, R.S. (2019). Chitosan coated calcium alginate beads for covalent immobilization of acrylamidase: Process parameters and removal of acrylamide from coffee. *Food Chemistry* ,*275* , 95-104. https://doi.org/10.1016/j.foodchem.2018.09.090

Bilal, M., Asgher, M., Cheng, H., Yan, Y., Iqbal, H.M.N. (2019). Multi-point enzyme immobilization, surface chemistry, and novel platforms: a paradigm shift in biocatalyst design. *Critical Reviews in Biotechnology* , *39* (2), 202-219. https://doi.org/10.1080/07388551.2018.1531822

Bilal, M., Iqbal, H.M.N. (2019). Naturally-derived biopolymers: Potential platforms for enzyme immobilization. *International Journal of Biological Macromolecules* , *130* , 462-482.

https://doi.org/10.1016/j.ijbiomac.2019.02.152

Cantone, S., Ferrario, V., Corici, L., Ebert, C., Fattor, D., Spizzo, P., Gardossi, L. (2013). Efficient immobilisation of industrial biocatalysts: criteria and constraints for the selection of organic polymeric carriers and immobilisation methods. *Chemical Society Reviews* , *42* (15), 6262-6276. https://doi.org/10.1039/c3cs35464d

Cheng, Y., Zheng, F., Lu, J., Shang, L., Xie, Z., Zhao, Y., Chen, Y., Gu, Z. (2014). Bioinspired Multicompartmental Microfibers from Microfluidics. *Advanced Materials* , *26* (30), 5184-5190. https://doi.org/10.1002/adma.201400798

Coppi, G., Iannuccelli, V., Leo, E., Bernabei, M.T., Cameroni, R. (2002). Protein immobilization in crosslinked alginate microparticles.*Journal of Microencapsulation* , *19* (1), 37-44. https://doi.org/10.1080/02652040110055621

Dong, Y.L., Zhang, H.G., Rahman, Z.U., Su, L., Chen, X.J., Hu, J., Chen, X.G. (2012). Graphene oxide-Fe_3O_4magnetic nanocomposites with peroxidase-like activity for colorimetric detection of glucose. *Nanoscale* , *4* (13), 3969-3976. https://doi.org/10.1039/c2nr12109c

El-Naggar, M.E., Abdel-Aty, A.M., Wassel, A.R., Elaraby, N.M., Mohamed, S.A. (2021). Immobilization of horseradish peroxidase on cationic microporous starch: Physico-bio-chemical characterization and removal of phenolic compounds. *International Journal of Biological Macromolecules* , *181* , 734-742. https://doi.org/10.1016/j.ijbiomac.2021.03.171

Felisardo, R.J.A., Luque, A.M., Silva, Q.S., Soares, C.M.F., Fricks, A.T., Lima, Á.S., Cavalcanti, E.B. (2020). Biosensor of horseradish peroxidase immobilized onto self-assembled monolayers: Optimization of the deposition enzyme concentration. *Journal of Electroanalytical Chemistry* , *879* , 114784. https://doi.org/10.1016/j.jelechem.2020.114784

Gao, Q., He, Y., Fu, J.Z., Liu, A., Ma, L. (2015). Coaxial nozzle-assisted 3D bioprinting with built-in microchannels for nutrients delivery. *Biomaterials* , *61* , 203-215. https://doi.org/10.1016/j.biomaterials.2015.05.031

Gejji, V., Fernando, S. (2018). Polyelectrolyte based technique for sequestration of protein from an aqueous phase to an organic solvent.*Separation and Purification Technology* , *207* , 68-76. https://doi.org/10.1016/j.seppur.2018.06.003

Grabovac, V., Laffleur, F., Bernkop-Schnürch, A. (2015). Thiomers: Influence of molecular mass and thiol group content of poly(acrylic acid) on efflux pump inhibition. *International Journal of Pharmaceutics* , *493* (1-2), 374-379. https://doi.org/10.1016/j.ijpharm.2015.05.079

Grant, J., Modica, J.A., Roll, J., Perkovich, P., Mrksich, M. (2018). An Immobilized Enzyme Reactor for Spatiotemporal Control over Reaction Products. *Small* , *14* (31), e1800923. https://doi.org/10.1002/smll.201800923

Gunatilake, U.B., Garcia-Rey, S., Ojeda, E., Basabe-Desmonts, L., Benito-Lopez, F. (2021). TiO_2 Nanotubes Alginate Hydrogel Scaffold for Rapid Sensing of Sweat Biomarkers: Lactate and Glucose. *ACS Applied Materials & Interfaces* , *13* (31), 37734-37745. https://doi.org/10.1021/acsami.1c11446

Hanefeld, U., Gardossi, L., Magner, E. (2009). Understanding enzyme immobilisation. *Chemical Society Reviews* , *38* (2), 453-468. https://doi.org/10.1039/b711564b

He, W., Gao, Y., Zhu, G., Wu, H., Fang, Z., Guo, K. (2020). Microfluidic synthesis of fatty acid esters: Integration of dynamic combinatorial chemistry and scale effect. *Chemical Engineering Journal* ,*381* , 122721. https://doi.org/10.1016/j.cej.2019.122721

Henderson, C.J., Pumford, E., Seevaratnam, D.J., Daly, R., Hall, E.A.H. (2019). Gene to diagnostic: Self immobilizing protein for silica microparticle biosensor, modelled with sarcosine oxidase.*Biomaterials* , *193* , 58-70. https://doi.org/10.1016/j.biomaterials.2018.12.003

Ho, W.F., Nguyen, L.T., Yang, K.L. (2019). A microfluidic sensor for detecting chlorophenols using cross-linked enzyme aggregates (CLEAs).*Lab on a Chip* , *19* (4), 634-640. https://doi.org/10.1039/c8lc01065j

Hu, C., Bai, Y.X., Hou, M., Wang, Y.S., Wang, L.C., Cao, X., Chan, C., Sun, H., Li, W.B., Ge, J., Ren, K.N. (2020). Defect-induced activity enhancement of enzyme-encapsulated metal-organic frameworks revealed in microfluidic gradient mixing synthesis. *Science Advances* ,*6* (5), eaax5785. https://doi.org/10.1126/sciadv.aax5785

Huang, Q., Li, Y., Fan, L., Xin, J.H., Yu, H., Ye, D. (2020). Polymorphic calcium alginate microfibers assembled using a programmable microfluidic field for cell regulation. *Lab on a Chip* ,*20* (17), 3158-3166. https://doi.org/10.1039/d0lc00517g

Jannat, M., Yang, K.L. (2020). A Millifluidic Device with Embedded Cross-Linked Enzyme Aggregates for Degradation of H_2O_2. *ACS Applied Materials & Interfaces* , *12* (5), 6768-6775. https://doi.org/10.1021/acsami.9b21480

Jeon, O., Bouhadir, K.H., Mansour, J.M., Alsberg, E. (2009). Photocrosslinked alginate hydrogels with tunable biodegradation rates and mechanical properties. *Biomaterials* , *30* (14), 2724-2734. https://doi.org/10.1016/j.biomaterials.2009.01.034

Jeong, W., Kim, J., Kim, S., Lee, S., Mensing, G., Beebe, D.J. (2004). Hydrodynamic microfabrication via "on the fly" photopolymerization of microscale fibers and tubes. *Lab on a Chip* , *4* (6), 576-580. https://doi.org/10.1039/b411249k

Ji, J., Joh, H.I., Chung, Y., Kwon, Y. (2017). Glucose oxidase and polyacrylic acid based water swellable enzyme-polymer conjugates for promoting glucose detection. *Nanoscale* , *9* (41), 15998-16004. https://doi.org/10.1039/c7nr05545e

Jun, Y., Kang, E., Chae, S., Lee, S.H. (2014). Microfluidic spinning of micro- and nano-scale fibers for tissue engineering. *Lab on a Chip* , *14* (13), 2145-2160. https://doi.org/10.1039/c3lc51414e

Kabernick, D.C., Gostick, J.T., Ward, V.C.A. (2022). Kinetic characterization and modeling of sequentially entrapped enzymes in 3D-printed PMMA microfluidic reactors for the synthesis of amorphadiene via the isopentenol utilization pathway. 1-13. *Biotechnology and Bioengineering* , https://doi.org/10.1002/bit.28046

Kahya, N., Erim, F.B. (2019). Surfactant modified alginate composite gels for controlled release of protein drug. *Carbohydrate Polymers* , *224* , 115165. https://doi.org/10.1016/j.carbpol.2019.115165

Kizilay, E., Seeman, D., Yan, Y., Du, X., Dubin, P.L., Donato-Capel, L., Bovetto, L., Schmitt, C. (2014). Structure of bovine beta-lactoglobulin-lactoferrin coacervates. *Soft Matter* ,*10* (37), 7262-7268. https://doi.org/10.1039/c4sm01333f

Ko, E., Tran, V.-K., Son, S.E., Hur, W., Choi, H., Seong, G.H. (2019). Characterization of Au@PtNP/GO nanozyme and its application to electrochemical microfluidic devices for quantification of hydrogen peroxide. *Sensors and Actuators B-Chemical* , *294* , 166-176. https://doi.org/10.1016/j.snb.2019.05.051

Lee, C., Lee, S.-Y. (2016). Preparation of colorimetric hydrogel beads for hydrofluoric acid detection. *Journal of Industrial and Engineering Chemistry* , *38* , 67-72. https://doi.org/10.1016/j.jiec.2016.04.006

Li, Y., Huang, Z.Z., Weng, Y., Tan, H. (2019). Pyrophosphate ion-responsive alginate hydrogel as an effective fluorescent sensing platform for alkaline phosphatase detection. *Chemical Communications* , *55* (76), 11450-11453. https://doi.org/10.1039/c9cc05223b

Liang, S., Wu, X.-L., Xiong, J., Zong, M.-H., Lou, W.-Y. (2020). Metal-organic frameworks as novel matrices for efficient enzyme immobilization: An update review. *Coordination Chemistry Reviews* ,*406* , 213149. https://doi.org/10.1016/j.ccr.2019.213149

Liese, A., Hilterhaus, L. (2013). Evaluation of immobilized enzymes for industrial applications. *Chemical Society Reviews* , *42* (15), 6236-6249. https://doi.org/10.1039/c3cs35511j

Lin, T., Zhong, L., Guo, L., Fu, F., Chen, G. (2014). Seeing diabetes: visual detection of glucose based on the intrinsic peroxidase-like activity of MoS_2 nanosheets. *Nanoscale* ,*6* (20), 11856-11862. https://doi.org/10.1039/c4nr03393k

Liu, D.-M., Chen, J., Shi, Y.-P. (2018). Advances on methods and easy separated support materials for enzymes immobilization. *Trends in Analytical Chemistry* , *102* , 332-342. https://doi.org/10.1016/j.trac.2018.03.011

Liu, H., Nidetzky, B. (2021). Leloir glycosyltransferases enabled to flow synthesis: Continuous production of the natural C-glycoside nothofagin. *Biotechnolgy and Bioengineering* , *118* (11), 4402-4413. https://doi.org/10.1002/bit.27908

Liu, X., Xue, P., Jia, F., Shi, K., Gu, Y., Ma, L., Li, R. (2021). A novel approach to efficient degradation of indole using co-immobilized horseradish peroxidase-syringaldehyde as biocatalyst.*Chemosphere* , *262* , 128411. https://doi.org/10.1016/j.chemosphere.2020.128411

Nie, B., Stutzman, J., Xie, A. (2005). A vibrational spectral maker for probing the hydrogen-bonding status of protonated Asp and Glu residues.*Biophysical Journal* , *88* (4), 2833-2847. https://doi.org/10.1529/biophysj.104.047639

Othman, R., Vladisavljević, G.T., Nagy, Z.K. (2015). Preparation of biodegradable polymeric nanoparticles for pharmaceutical applications using glass capillary microfluidics. *Chemical Engineering Science* , *137* , 119-130. https://doi.org/10.1016/j.ces.2015.06.025

Pawar, S.N., Edgar, K.J. (2012). Alginate derivatization: a review of chemistry, properties and applications. *Biomaterials* ,*33* (11), 3279-3305. https://doi.org/10.1016/j.biomaterials.2012.01.007

Qin, Y. (2008). Alginate fibres: an overview of the production processes and applications in wound management. *Polymer International* ,*57* (2), 171-180. https://doi.org/10.1002/pi.2296

Ren, S., Li, C., Jiao, X., Jia, S., Jiang, Y., Bilal, M., Cui, J. (2019). Recent progress in multienzymes co-immobilization and multienzyme system applications. *Chemical Engineering Journal* ,*373* , 1254-1278. https://doi.org/10.1016/j.cej.2019.05.141

Riccardi, C.M., Cole, K.S., Benson, K.R., Ward, J.R., Bassett, K.M., Zhang, Y., Zore, O.V., Stromer, B., Kasi, R.M., Kumar, C.V. (2014). Toward "stable-on-the-table" enzymes: improving key properties of catalase by covalent conjugation with poly(acrylic acid).*Bioconjugate Chemistry* , *25* (8), 1501-1510. https://doi.org/10.1021/bc500233u

Rudroff, F., Mihovilovic, M.D., Gröger, H., Snajdrova, R., Iding, H., Bornscheuer, U.T. (2018). Opportunities and challenges for combining chemo- and biocatalysis. *Nature Catalysis* , *1* (1), 12-22. https://doi.org/10.1038/s41929-017-0010-4

Secundo, F. (2013). Conformational changes of enzymes upon immobilisation. *Chemical Society Reviews* , *42* (15), 6250-6261. https://doi.org/10.1039/c3cs35495d

Shao, L., Gao, Q., Xie, C., Fu, J., Xiang, M., He, Y. (2019). Bioprinting of Cell-Laden Microfiber: Can It Become a Standard Product?*Advanced Healthcare Materials* , *8* (9), e1900014. https://doi.org/10.1002/adhm.201900014

Shao, L., Gao, Q., Zhao, H., Xie, C., Fu, J., Liu, Z., Xiang, M., He, Y. (2018). Fiber-Based Mini Tissue with Morphology-Controllable GelMA Microfibers. *Small* , *14* (44), e1802187. https://doi.org/10.1002/smll.201802187

Sheldon, R.A., van Pelt, S. (2013). Enzyme immobilisation in biocatalysis: why, what and how. *Chemical Society Reviews* ,*42* (15), 6223-6235. https://doi.org/10.1039/c3cs60075k

Shin, S., Park, J.Y., Lee, J.Y., Park, H., Park, Y.D., Lee, K.B., Whang, C.M., Lee, S.H. (2007). "On the fly" continuous generation of alginate fibers using a microfluidic device. *Langmuir* , *23* (17), 9104-9108.

https://doi.org/10.1021/la700818q

Singh, S., Mitra, K., Singh, R., Kumari, A., Sen Gupta, S.K., Misra, N., Maiti, P., Ray, B. (2017). Colorimetric detection of hydrogen peroxide and glucose using brominated graphene. *Analytical Methods* ,*9* (47), 6675-6681. https://doi.org/10.1039/c7ay02212c

Singh, S., Singh, A., Bais, V.S., Prakash, B., Verma, N. (2014). Multi-scale carbon micro/nanofibers-based adsorbents for protein immobilization. *Materials Science and Engineering C* , *38* , 46-54. https://doi.org/10.1016/j.msec.2014.01.042

Teepakorn, C., Zajkoska, P., Cwicklinski, G., De Berardinis, V., Zaparucha, A., Nonglaton, G., Anxionnaz-Minvielle, Z. (2021). Nitrilase immobilization and transposition from a micro-scale batch to a continuous process increase the nicotinic acid productivity.*Biotechnology Journal* , *16* (10), e2100010. https://doi.org/10.1002/biot.202100010

Todea, A., Benea, I.C., Bîtcan, I., Péter, F., Klébert, S., Feczkó, T., Károly, Z., Biró, E. (2021). One-pot biocatalytic conversion of lactose to gluconic acid and galacto-oligosaccharides using immobilized β-galactosidase and glucose oxidase. *Catalysis Today* , *366* , 202-211. https://doi.org/10.1016/j.cattod.2020.06.090

Wang, X., Zhu, K.X., Zhou, H.M. (2011). Immobilization of glucose oxidase in alginate-chitosan microcapsules. *International Journal of Molecular Sciences* , *12* (5), 3042-3054. https://doi.org/10.3390/ijms12053042

Wu, X., Yang, C., Ge, J., Liu, Z. (2015). Polydopamine tethered enzyme/metal-organic framework composites with high stability and reusability. *Nanoscale* , *7* (45), 18883-18886. https://doi.org/10.1039/c5nr05190h

Yang, H., Guo, M. (2019). Bioinspired Polymeric Helical and Superhelical Microfibers via Microfluidic Spinning. *Macromolecular Rapid Communication* , *40* (12), e1900111. https://doi.org/10.1002/marc.201900111

Yang, J., Li, J., Ng, D.H.L., Yang, P., Yang, W., Liu, Y. (2020). Micromotor-assisted highly efficient Fenton catalysis by a laccase/Fe-BTC-$NiFe_2O_4$ nanozyme hybrid with a 3D hierarchical structure. *Environmental Science Nano* ,*7* (9), 2573-2583. https://doi.org/10.1039/c9en01443h

Yu, Y., Fu, F., Shang, L., Cheng, Y., Gu, Z., Zhao, Y. (2017). Bioinspired Helical Microfibers from Microfluidics. *Advanced Materials* , *29* (18), 1605765. https://doi.org/10.1002/adma.201605765

Yu, Y., Shang, L., Guo, J., Wang, J., Zhao, Y. (2018). Design of capillary microfluidics for spinning cell-laden microfibers.*Nature Protocols* , *13* (11), 2557-2579. https://doi.org/10.1038/s41596-018-0051-4

Zanker, A.A., Ahmad, N., Son, T.H., Schwaminger, S.P., Berensmeier, S. (2021). Selective ene-reductase immobilization to magnetic nanoparticles through a novel affinity tag. *Biotechnology Journal* ,*16* (4), e2000366. https://doi.org/10.1002/biot.202000366

Zdarta, J., Meyer, A., Jesionowski, T., Pinelo, M. (2018). A General Overview of Support Materials for Enzyme Immobilization: Characteristics, Properties, Practical Utility. *Catalysts* ,*8* (2), 92. https://doi.org/10.3390/catal8020092

Zhang, D.M., Vangala, K., Jiang, D.P., Zou, S.G., Pechan, T. (2010). Drop Coating Deposition Raman Spectroscopy of Fluorescein Isothiocyanate Labeled Protein. *Applied Spectroscopy* , *64* (10), 1078-1085. https://doi.org/10.1366/000370210792973497

Zhang, Y., Ge, J., Liu, Z. (2015). Enhanced Activity of Immobilized or Chemically Modified Enzymes. *ACS Catalysis* , *5* (8), 4503-4513. https://doi.org/10.1021/acscatal.5b00996

Zhou, Z., Hartmann, M. (2013). Progress in enzyme immobilization in ordered mesoporous materials and related applications. *Chemical Society Reviews* , *42* (9), 3894-3912. https://doi.org/10.1039/c3cs60059a

Zhu, K., Yu, Y., Cheng, Y., Tian, C., Zhao, G., Zhao, Y. (2019a). All-Aqueous-Phase Microfluidics for Cell Encapsulation. *ACS Applied Materials & Interfaces* , *11* (5), 4826-4832.

https://doi.org/10.1021/acsami.8b19234

Zhu, Y., Huang, Z., Chen, Q., Wu, Q., Huang, X., So, P.K., Shao, L., Yao, Z., Jia, Y., Li, Z., Yu, W., Yang, Y., Jian, A., Sang, S., Zhang, W., Zhang, X. (2019b). Continuous artificial synthesis of glucose precursor using enzyme-immobilized microfluidic reactors. *Nature Communications* , *10* (1), 4049. https://doi.org/10.1038/s41467-019-12089-6

Zore, O.V., Pande, P., Okifo, O., Basu, A.K., Kasi, R.M., Kumar, C.V. (2017). Nanoarmoring: strategies for preparation of multi-catalytic enzyme polymer conjugates and enhancement of high temperature biocatalysis. *RSC Advances* , *7* (47), 29563-29574. https://doi.org/10.1039/c7ra05666d